Theoretical study of the conductance of ferromagnetic atomic-sized contacts

M. Häfner,[1,2] J. K. Viljas,[1,3] D. Frustaglia,[4] F. Pauly,[1,3] M. Dreher,[5] P. Nielaba,[5] and J. C. Cuevas[2,1,3]
[1]*Institut für Theoretische Festkörperphysik, Universität Karlsruhe, D-76128 Karlsruhe, Germany*
[2]*Departamento de Física Teórica de la Materia Condensada, Universidad Autónoma de Madrid, E-28049 Madrid, Spain*
[3]*Institut für Nanotechnologie, Forschungszentrum Karlsruhe, D-76021 Karlsruhe, Germany*
[4]*NEST-CNR-INFM and Scuola Normale Superiore, I-56126 Pisa, Italy*
[5]*Fachbereich Physik, Universität Konstanz, D-78457 Konstanz, Germany*
(Received 5 February 2008; published 10 March 2008)

In this work, we study theoretically the conductance of atomic contacts of the ferromagnetic 3*d* materials Fe, Co, and Ni. For this purpose, we employ a tight-binding model and we focus on the analysis of ideal contact geometries. In agreement with previous theoretical results, the 3*d* bands of these transition metals play the key role in the electrical conduction of atomic contacts. As a consequence, in the contact regime, there are partially open conductance channels and the conductance of the last plateau is typically above $G_0=2e^2/h$. Furthermore, in this regime, there is no complete spin polarization of the current (i.e., both spin bands contribute to transport) and the amplitude of the conductance as well as its spin polarization are very sensitive to disorder in the contact geometry. Finally, we find that in the tunneling regime, a high spin polarization of the current can be achieved.

DOI: 10.1103/PhysRevB.77.104409 PACS number(s): 75.75.+a, 73.63.Rt

I. INTRODUCTION

Metallic nanowires fabricated by means of scanning-tunneling microscope and break-junction techniques have turned out to be a unique playground to test the basic concepts of electronic transport at the atomic scale.[1] In the case of nonmagnetic materials, the zero-bias conductance of such contacts is described by the Landauer formula $G=G_0\Sigma_n T_n$. Here, the sum runs over all the available conduction channels, T_n is the transmission for the nth channel, and the quantum of conductance G_0 is defined as $G_0=2e^2/h$. It has been shown that the number of channels in a one-atom contact is mainly determined by the number of valence orbitals of the central atom, and the transmission of each channel is fixed by the local atomic environment.[2–4] Thus, for instance, a one-atom contact of a monovalent metal such as Au sustains a single channel, while for *sp*-like metals such as Al or Pb, one finds three channels due to the contribution of the *p* orbitals. More importantly, for the discussion in this work, in a transition metal such as Nb the contribution of the *d* orbitals leads to five partially open channels.[2,3,5] In the case of ferromagnetic materials, the spin symmetry is broken. In the description of the conductance, one should then replace G_0 by $G_0/2=e^2/h$ and include a sum over spins in the Landauer formula.

In the past years, a lot of attention has been devoted to the experimental[6–30] and theoretical[31–48] analysis of contacts of the 3*d* ferromagnetic materials. In particular, several experimental groups have analyzed the conductance histograms of these materials. Basically, two contradictory results have been reported. On the one hand, several groups have observed peaks in the conductance histogram at half-integer multiples of G_0.[17–22] This has been interpreted as a manifestation of half-integer conductance quantization,[20] implying that only fully open channels contribute to the conductance. In this sense, a peak at $0.5G_0$ would then additionally mean the existence of a full spin polarization of the current. Furthermore, some authors have reported conductance histograms that are very sensitive to an external magnetic field.[11]

On the other hand, Untiedt *et al.*[23] have measured the conductance for atomic contacts of the 3*d* ferromagnetic metals (Fe, Co, and Ni) using break junctions under cryogenic vacuum conditions. Contrary to the experiments mentioned above, they have reported the absence of fractional conductance quantization, even when a high external magnetic field was applied. Instead, they observe conductance histograms that show broad peaks above $1G_0$, with only little weight below it, which is generally expected for transition metals.[15,49]

In order to resolve the contradiction of the experimental results about the existence of half-integer conductance quantization, several authors have already investigated theoretically the electronic structure and conductance of nanocontacts of the 3*d* ferromagnetic metals. Most of the work has been focused on the accurate *ab initio* description of the electronic structure of ideal systems.[33,34,37–39,42–44,46,48] In the case of monatomic wires, different aspects such as the influence of a domain wall on the electronic structure,[33] the effect of electronic correlations,[39] or the magnetic properties[47] have been discussed. The conduction properties of ideal atomic-contact geometries have also been investigated both with *ab initio* methods[37,38,42–44,46,48] and tight-binding models for the case of Fe atomic contacts and wires.[40,50] Based on these studies, one would not expect either conductance quantization or full spin polarization in ferromagnetic atomic contacts.

In this work, we analyze the conductance of atomic contacts of the 3*d* ferromagnetic materials (Fe, Co, and Ni). Our goal is to provide further insight into basic issues such as the orbitals relevant for the electron transport, the role of atomic disorder, the dependence of the spin polarization of the current on the contact geometry, and the main differences between these three materials. For this purpose, we have analyzed ideal geometries of few-atom contacts, assuming them to form a single magnetic domain. To describe the electronic

structure, we use a tight-binding model, while the conductance calculations are based on Green's function techniques. The parameters of the model are obtained by fitting the bulk band structure to *ab initio* calculations[51] and, thus, their use for the description of nanocontacts might be questionable. We partially correct this problem by modifying the parameters to enforce local charge neutrality in the atoms of nanoconstrictions. Despite the limitations of this procedure, the method has been very successful in explaining the most important features of the experimental results for nonmagnetic metallic atomic contacts.[2,4,52,53] Moreover, by combining it with independent structural simulations, it allows one to address important issues presently out of the scope of *ab initio* approaches, such as the interplay between mechanical and electronic properties in conductance histograms.[54,55] In this paper, we study the influence of variations in the atomic positions on the conductance by considering random disorder in the ideal geometries.

The results of our calculations for the three materials can be summarized as follows: Due to the partially open conduction channels of the minority spin electrons, there is, in general, no conductance quantization and the conductance of the last plateau has a value typically above $G_0=2e^2/h$. In the contact regime, both spin species contribute to the transport and the current is never fully spin polarized. Furthermore, the values of the conductance and the current polarization are very sensitive to the contact geometry and disorder. The origin of all these findings can be traced back to the fact that the d bands of these transition metals play an important role in the electrical conduction. Finally, we find that in the tunneling regime, which is reached when the contacts are broken, the nature of the conduction changes qualitatively. In this case, almost fully spin-polarized currents are, indeed, possible.

The rest of the paper is organized as follows. In the following section, we describe our tight-binding approach to compute the conductance of the ferromagnetic atomic contacts. Section III is devoted to the analysis of the results of the conductance of representative one-atom-thick contacts of Fe, Co, and Ni. Moreover, we include in this section a discussion of the conductance in the tunneling regime. In Sec. IV, we discuss the influence of atomic disorder on the conductance of single-atom contacts. Finally, in Sec. V, we summarize and discuss the main results.

II. DESCRIPTION OF THE THEORETICAL MODEL

Our goal is to compute the low-temperature linear conductance of atomic-sized contacts of the $3d$ ferromagnetic metals Fe, Co, and Ni. For this purpose, we use a tight-binding model based on the sophisticated parametrization introduced in Ref. 51. Such tight-binding models have been successful in the description of electron transport in metallic atomic contacts.[2,4,52] Our approach follows closely the one used in Refs. 53, 54, and 56, and we now proceed to describe it briefly.

In our approach, the electronic structure of the atomic contacts is described in terms of the following tight-binding Hamiltonian written in a nonorthogonal basis

$$\hat{H} = \sum_{i\alpha,j\beta,\sigma} H^{\sigma}_{i\alpha,j\beta} \hat{c}^{\dagger}_{i\alpha,\sigma} \hat{c}_{j\beta,\sigma}. \tag{1}$$

Here, i,j run over the atomic sites, α,β denote the different atomic orbitals, and $\sigma=\uparrow,\downarrow$ denotes the spin. Furthermore, $H^{\sigma}_{i\alpha,j\beta}$ for $i=j$ and $\alpha=\beta$ are the spin-dependent on-site energies, and for $i\neq j$ the hopping elements, while $H^{\sigma}_{i\alpha,i\beta}=0$ for $\alpha\neq\beta$. In addition, we need the overlaps between the different orbitals, $S_{i\alpha,j\beta}$, which are spin independent. We take all these parameters from the bulk parametrization of Ref. 51, which is known to accurately reproduce the band structure and total energy of bulk ferromagnetic materials.[57] Notice that in our model, there is no mixing of the two spin species, which means that, in particular, we do not consider spin-orbit interaction. The atomic basis is formed by nine orbitals $(3d,4s,4p)$, which give rise to the main bands around the Fermi energy in Fe, Co, and Ni. It is important to emphasize that in this parametrization both the hopping elements and the overlaps are functions of the relative positions of the atoms, which allows us to study also geometrical disorder. These functions have a cutoff radius that encloses atoms well beyond the tenth nearest neighbors in a bulk geometry for Fe, Co, and Ni.

In order to compute the linear conductance, we apply a standard Green's function method.[2,52–54,56] For this, we divide the system into three parts, the left (L) and right (R) leads, and the central cluster (C) containing the constriction. In this way, the retarded central cluster Green's functions, $\mathbf{G}^{\sigma}_{CC}$, are given by

$$\mathbf{G}^{\sigma}_{CC}(E) = [E\mathbf{S}_{CC} - \mathbf{H}^{\sigma}_{CC} - \mathbf{\Sigma}^{\sigma}_{L}(E) - \mathbf{\Sigma}^{\sigma}_{R}(E)]^{-1}. \tag{2}$$

Here, $\mathbf{H}^{\sigma}_{CC}$ and $\mathbf{S}_{CC}$ are the Hamiltonian and the overlap matrix of the central cluster, respectively, and $\mathbf{\Sigma}^{\sigma}_{L/R}$ are the self-energies, which contain the information of the electronic structure of the leads and their coupling to the central part of the contact. These self-energies can be expressed as

$$\mathbf{\Sigma}^{\sigma}_{L}(E) = (\mathbf{H}^{\sigma}_{CL} - E\mathbf{S}_{CL})\mathbf{g}^{\sigma}_{LL}(E)(\mathbf{H}^{\sigma}_{LC} - E\mathbf{S}_{LC}), \tag{3}$$

with a similar equation for $\mathbf{\Sigma}^{\sigma}_{R}(E)$. Here, for example, $\mathbf{H}^{\sigma}_{CL}$ is the hopping matrix connecting the central cluster C and the lead L, $\mathbf{S}_{CL}$ is the corresponding block of the overlap matrix, and $\mathbf{g}^{\sigma}_{LL}(E)$ is the retarded Green's function of the uncoupled lead. Both infinite leads are described by ideal surfaces, the Green's functions of which are calculated within the same tight-binding parametrization using the decimation technique described in Ref. 58.

In an atomic contact, the local environment in the region of the constriction is very different from that of the bulk material. In particular, this fact can lead to large deviations from the approximate local charge neutrality that typical metallic elements exhibit. We correct this problem by imposing charge neutrality on all the atoms of the nanowire through a self-consistent variation of $\mathbf{H}^{\sigma}_{CC}$, following Ref. 56 and shifting both spin species equally.

The linear conductance at low temperature can now be expressed in terms of the Landauer formula

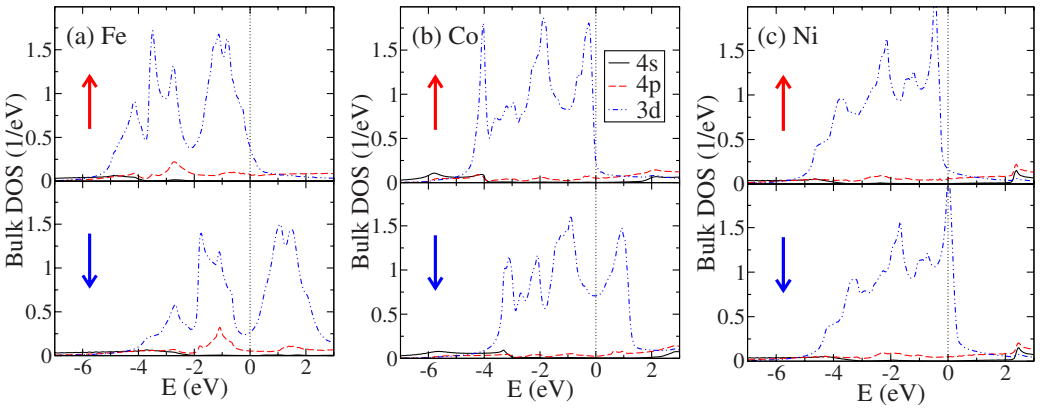

FIG. 1. (Color online) Bulk DOS of Fe, Co, and Ni, resolved with respect to the individual contributions of 3*d*, 4*s*, and 4*p* orbitals, as indicated in the legend. Furthermore, the upper panels show the DOS for the majority spins and the lower ones the DOS for minority spins. The Fermi energy is set to zero and is indicated by the vertical dashed line.

$$G = \frac{e^2}{h} \sum_{\sigma} T_{\sigma}(E_F), \tag{4}$$

where $T_\sigma(E)$ is the total transmission for spin $\sigma=\uparrow,\downarrow$ at energy E, and E_F is the Fermi energy. We also define the spin-resolved conductances $G_\sigma=(e^2/h)T_\sigma(E_F)$, such that $G=G_\uparrow+G_\downarrow$. The transmissions are obtained as follows:

$$T_{\sigma}(E) = \mathrm{Tr}[\mathbf{t}_{\sigma}(E)\mathbf{t}_{\sigma}^{\dagger}(E)] = \sum_{n} T_{n,\sigma}(E), \tag{5}$$

where $\mathbf{t}_\sigma(E)$ is the transmission matrix and $T_{n,\sigma}(E)$ are the individual transmission eigenvalues for each spin σ. The transmission matrix can be calculated in terms of the Green's functions $\mathbf{G}^{\sigma}_{CC}$ as follows:

$$\mathbf{t}_{\sigma}(E) = 2[\mathbf{\Gamma}^{\sigma}_{L}(E)]^{1/2}\mathbf{G}^{\sigma}_{CC}(E)[\mathbf{\Gamma}^{\sigma}_{R}(E)]^{1/2}. \tag{6}$$

Here, $\Gamma^\sigma_{L/R}(E)$ are the scattering rate matrices given by $\Gamma^\sigma_{L/R}(E)=-\mathrm{Im}[\mathbf{\Sigma}^\sigma_{L/R}(E)]$.

III. CONDUCTANCE OF IDEAL SINGLE-ATOM CONTACTS OF Fe, Co, AND Ni

The goal of this section is the analysis of the conductance of ideal, yet plausible one-atom contact geometries for the three ferromagnetic metals (Fe, Co, and Ni) considered in this work. In order to understand the results described below, it is instructive to first discuss the bulk density of states (DOS). The spin- and orbital-resolved bulk DOS of these materials around E_F, as calculated from our tight-binding model, is shown in Fig. 1. The common feature for the three ferromagnets is that the Fermi energy for the minority spins lies inside the *d* bands. This fact immediately suggests[2,3] that the *d* orbitals may play an important role in the transport. The occupation of the *s* and *p* orbitals for both spins is around 0.25 and 0.4 electrons, respectively. For the majority spins, the Fermi energy lies close to the edge of the *d* band. The main difference between the materials is that for Fe there is still an important contribution of the *d* orbitals, while for Ni, the Fermi level is in a region where the *s* and *p* bands become more important. The calculated values of the magnetic moment per atom (in units of the Bohr magneton) of 2.15 for Fe, 1.3 for Co, and 0.45 for Ni are reasonably close to literature values.[59]

We now proceed to analyze in detail the conductance of some ideal one-atom geometries, which are chosen to simulate what happens in the last conductance plateau before the breaking of the nanowires. First, we consider the one-atom contacts shown in the upper panels of Fig. 2. These geometries are constructed starting with a single atom and choosing the nearest neighbors in the next layers of the ideal lattice along the direction indicated with an arrow. In the case of Fig. 2, for Fe (bcc lattice with a lattice constant of 2.86 Å) the contact is grown along the [001] direction, for Co (hcp lattice, lattice constant 2.51 Å) along the [001] direction (parallel to "*c* axis"), and for Ni (fcc lattice and lattice constant 3.52 Å) along the [111] direction. The number of atoms in the central region has been chosen large enough, such that the transmission does not depend anymore on the number of layers included. Moreover, as explained in the previous section, the central region is coupled seamlessly to ideal surfaces grown along the same direction.

Let us start describing the results for the Fe one-atom contact of Fig. 2(a). There, we present the total transmission for majority spins and minority spins as a function of energy as well as the individual transmissions. We find for this particular geometry the spin-resolved conductances $G_\uparrow=3.70e^2/h$ ($\uparrow$ for majority spins) and $G_\downarrow=3.75e^2/h$ ($\downarrow$ for minority spins), which result in a total conductance of $3.7G_0$. The conductance $G_\uparrow$ for the majority spins is the result of up to 8 open channels (with a transmission higher than 0.01), while for the minority spins, there are 11 channels giving a significant contribution to $G_\downarrow$. The large number of channels and, consequently, the high conductance are partially due to the large apex angle of 71° of the pyramids. As a consequence, the layers next to the central atom couple to each other and give rise to a significant tunneling current that proceeds directly without traversing the central atom. On the other hand, the larger number of channels for the minority spins is due to the key contribution of the *d* orbitals that dominate the transport through this spin species, while for

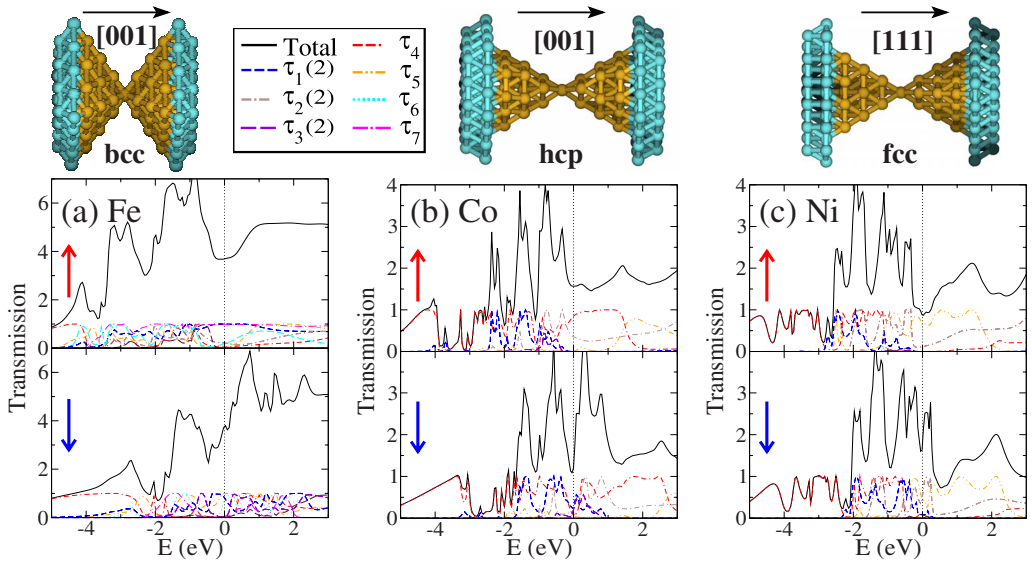

FIG. 2. (Color online) Transmission as a function of energy for the three single-atom contacts of (a) Fe, (b) Co, and (c) Ni, which are shown in the upper panels. We present the total transmission (black solid line) for both majority spins and minority spins as well as the transmission of individual conduction channels that give the most important contribution at Fermi energy, which is indicated by a vertical dotted line. The blue, brown, and violet dash-dotted lines of τ_1, τ_2, and τ_3 refer to twofold degenerate conduction channels. The legends in the upper graphs indicate in which direction the contacts are grown. These contacts contain in the central region 59 atoms for Fe, 45 for Co, and 39 for Ni. The blue atoms represent a part of the atoms of the leads (semi-infinite surfaces) that are coupled to the central atoms in our model.

the majority spins, the *s* and *p* orbitals are the more relevant ones. This fact, which is supported by the analysis of the local density of states (not shown here), is a simple consequence of the position of the Fermi energy and the magnitude of the spin splitting (see discussion of the bulk DOS above).

We define the spin polarization P of the current as

$$P = \frac{G_\uparrow - G_\downarrow}{G_\uparrow + G_\downarrow}. \tag{7}$$

With this definition, we find a value of $P=-0.7\%$ for the Fe one-atom contact of Fig. 2(a).

In order to compare to the polarization of the bulk, we have calculated the transmission at the Fermi energy for a series of contact geometries where a bar of constant diameter bridges the two lead surfaces. When the diameter of the bar (or central region of the contact) is increased, the polarization grows continuously and saturates at a value of $P=+40\%$ for a contact containing 219 atoms in 7 layers. This is in good agreement with the experimental value obtained using normal-metal-superconductor point contacts.[62] Notice that P can be quite different in an atomic contact as compared to the bulk. This is because the conductance is not simply controlled by the DOS at the Fermi energy, but the precise coupling between the orbitals in the constriction plays a crucial role.

For the Co contact depicted in Fig. 2(b), the transmission is lower than for Fe, partly due to the smaller apex angle of the hcp pyramids. In this case, we find $G_\uparrow=1.57e^2/h$ for majority spins and $G_\downarrow=1.21e^2/h$ for minority spins, summing up to a total conductance of $1.4G_0$. There are three channels contributing to $G_\uparrow$ and eight channels to $G_\downarrow$. As in the case of Fe, the larger number of channels for the minority spins is due to the position of the Fermi level and the resulting contribution of the *d* orbitals for this spin. We also find that there is a small but non-negligible contribution of channels that proceed directly without crossing the central atom. This explains, in particular, why one has eight channels for the minority spins, although at most six bands (*s* and *d*) have a significant DOS at this energy. Turning to the current polarization, we find a value of $P=+13\%$ for the Co one-atom contact. We also calculate the polarization for a series of Co bars with increasing diameter in hcp [001] direction. As the diameter increases, the polarization decreases to a value of $P=-41\%$ for a contact containing five layers of 37 atoms each, again in good agreement with the experiment.[62] Notice again that not only the magnitude of P for a one-atom contact can be quite different from the bulk, but also its sign can be the opposite.

Finally, the Ni contact shown in Fig. 2(c) exhibits conductances of $G_\uparrow=0.85e^2/h$ for majority and $G_\downarrow=1.80e^2/h$ for minority spins, adding up to a total conductance of $1.3G_0$. The $G_\uparrow$ consists of three channels, due to the contribution of the *s* and *p* orbitals, and $G_\downarrow$ contains six channels, which originate from the contribution of the *d* orbitals. In this case, we find a value for the polarization of $P=-34\%$. Once more, we have investigated the polarization of bulk Ni in a series of large Ni bars in fcc [111] direction. Interestingly, the polarization decreases from $P=+3\%$ for a contact of 28 atoms in four layers to $P=-41\%$ for a contact consisting of 244 atoms in four layers.

Now we turn to the analysis of the geometries shown in the upper panels of Fig. 3. The difference with respect to the

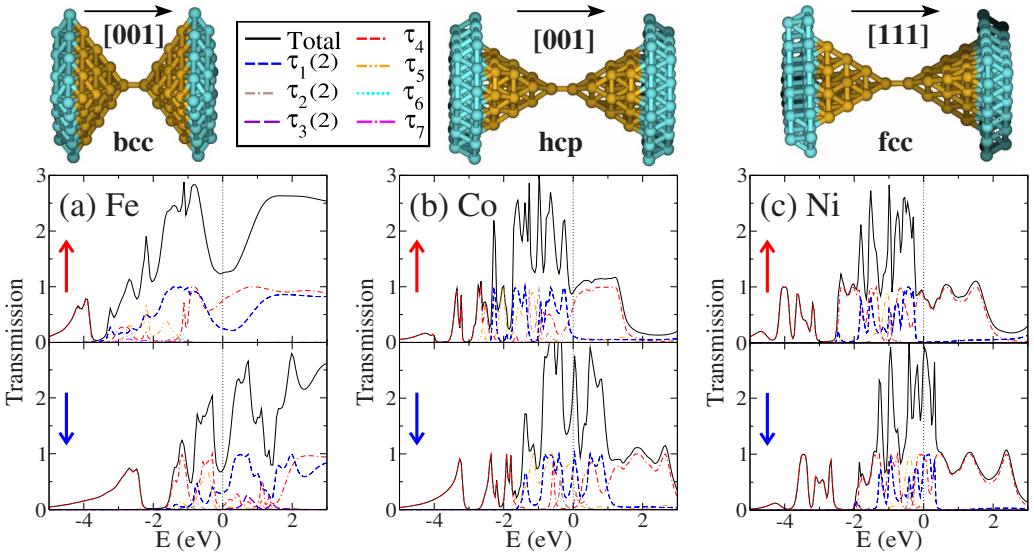

FIG. 3. (Color online) The same as in Fig. 2, but for the geometries shown in the upper graphs, which contain a dimer in the central part of the contact. The two dimer atoms are at the bulk nearest neighbor distance from each other.

geometries of Fig. 2 is the presence of a dimer in the central part of the contacts. This type of geometry has frequently been observed in molecular dynamics simulations of atomic contacts of Al (Ref. 61) and Au (Ref. 54), and we also find them in our simulations of Ni contacts in the last stages of the breaking process.[55]

Inserting a dimer with an atom separation equal to the bulk nearest neighbor distance in the geometries of Fig. 2 results in a larger separation of the pyramids to the left and right of the central atom and, therefore, in a weaker coupling between the layers next to the dimer. This is particularly important in the case of Fe. The resulting transmission for the Fe contact with a central dimer is shown in Fig. 3(a), where one can see that only three channels remain for the majority spins, yielding $G_{\uparrow}=1.24e^2/h$, while for the minority spins, three channels contribute to $G_{\downarrow}=0.70e^2/h$. The total conductance is $1.0G_0$ and the polarization $P=+28\%$. For Co, the contact of Fig. 3(b) with a central dimer exhibits $G_{\uparrow}=0.90e^2/h$ and $G_{\downarrow}=2.23e^2/h$, summing up to a total conductance of $1.6G_0$. The transmission is formed by three channels for the majority spins (with one clearly dominant) and six channels for minority spins and polarization is $P=-42\%$. Finally, for the Ni contact in Fig. 3(c) with a central dimer, a single channel contributes to $G_{\uparrow}=0.86e^2/h$ and four channels add up to $G_{\downarrow}=2.66e^2/h$. This means that one has a total conductance of $1.8G_0$, while the current polarization adopts a value of $P=-51\%$.

Beyond the precise numerical values detailed in the previous paragraph, we would like to stress the following conclusions from the analysis of Fig. 3. First, the transport contribution of the minority spins is dominated by the *d* orbitals, which give rise to several channels (from 3 to 5 depending on the material). Second, for the majority spins, there is a smaller number of channels ranging from 3 for Fe to 1 for Ni. This contribution is dominated by the *d* and *s* orbitals for Fe and only by the *s* orbitals for Co and Ni. The relative contribution and number of channels of the two spin species is a simple consequence of the position of the Fermi level and the magnitude of the spin splitting. In particular, notice that as we move from Fe to Ni, the Fermi energy lies more and more outside of the *d* band for the majority spins, which implies that the number of channels is reduced for this spin species. In particular, for Ni, a single majority spin channel dominates. On the other hand, notice that the conductance values for the different contacts lie typically above G_0, which is precisely what is observed experimentally.[23]

So far, we have analyzed geometries for the so-called contact regime where the nanowires are formed. As shown above, in this case, the contribution of the *d* bands makes it difficult to obtain large values of the current polarization. In this sense, one may wonder what happens in the tunneling regime when the contact is broken. In order to address this issue, we have simulated the breaking of the contacts by progressively separating the electrodes of the dimer geometries of Fig. 3. In this way, we have computed the conductance and the current polarization as a function of the tip separation *D*, and the results for the three materials are summarized in Fig. 4. With increasing *D*, one enters the tunneling regime, which is characterized by an exponential decay of the conductance. In the regime shown in Fig. 4, Fe does not yet exhibit an exponential decay. In contrast, the conductances for Co and Ni are well fitted by an exponential $\exp(-\beta D)$ with $\beta=2.3$ Å^{-1} and $\beta=1.9$ Å^{-1}, respectively. These values are in reasonable agreement with the Wentzel–Kramers–Brillouin approximation,[60] which yields $\beta=2.2$ Å^{-1} by using a work function of 5 eV.[59] Notice that deep in the tunneling regime for the three materials, the conductance for the majority spins largely overcomes the value of the minority spin conductance. This results in positive values of the current polarization *P* and, in particular, for Co and Ni, it reaches values very close to 100%.

The origin of these huge values of current polarization in the tunneling regime is the following. In this regime, the current is, roughly speaking, a convolution of the local den-

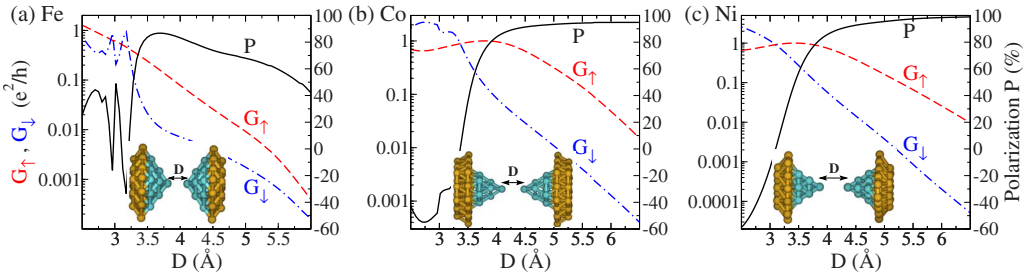

FIG. 4. (Color online) Conductance over tip separation D of similar geometries as in Fig. 3. The conductances of majority spin ($G_\uparrow$, dashed lines and left scales) and minority spin ($G_\downarrow$, dash-dotted lines and left scales) are shown, together with the resulting current polarization (solid lines and right scales).

sities of states on the tips weighted with the squared hoppings of the relevant orbitals of both electrodes. The hoppings between 3*d* orbitals decay faster with the separation of the tips than the corresponding hoppings of the 4*s* orbitals. Due to this faster decay, the conduction is then dominated by the *s* orbitals and, since the on-site energy for the minority spins lies further away from the Fermi energy than the corresponding one for majority spin, the transmission through the latter one is much higher, giving rise to a very large positive spin polarization P in the tunneling regime.

IV. ROLE OF ATOMIC DISORDER

In the previous section, we have seen that the 3*d* orbitals play an important role in transport. These orbitals are rather localized on the atoms and the energy bands that they give rise to have relatively flat dispersion relations. Therefore, one would expect the contribution of these orbitals to the transport to be very sensitive to the contact geometry. Indeed, in the previous section, we have seen examples in which, by changing the structure of the central part of the contacts, one can even change the sign of the current polarization. Motivated by these results, in this section, we study in a more systematic manner how the disorder in the atomic positions influences the conductance of one-atom contacts.

In order to simulate the role of disorder, we have studied the conductance of contacts, in which the atomic positions in the central cluster have been changed randomly using the geometries of Figs. 2 and 3 as starting points. In Fig. 5, we present an example of such a study, where we show histograms of the channel-resolved transmissions at the Fermi energy $T_{n,\sigma}(E_F)$ for both spins σ constructed from around 3000 realizations of disorder for each contact. The amplitude of the random displacement in each direction was, in this case, 0.05 times the lattice constant. Similar results for contacts of the noble metal Au are also shown for comparison. Moreover, for the ferromagnetic materials, the insets show corresponding histograms of the spin polarization P of the current.

Let us now discuss the main features of the transmission histograms. First, they show that the number of channels obtained for the ideal geometries in the previous section is robust with respect to disorder, although the transmission coefficients depend crucially on the precise atomic positions. Second, for the minority spins, one has a non-negligible contribution of at least five channels, which originate mainly from the *d* bands. For the majority spins, the number of channels is clearly smaller and is progressively reduced as we go from Fe to Ni. This is particularly obvious in the panels of the dimer structures, where one can see that for Fe, there are three sizable channels and the contribution of the smallest two decreases for Co and Ni. As explained in the previous section, this is a consequence of the relative position of the Fermi energy in these three metals. For the latter case of Ni, one channel clearly dominates the majority spin conductance, but second and third channels are still present. Thus, unlike in the case of noble metals such as Au, which only have a single channel (see Fig. 5), for ferromagnetic materials, conductance quantization is not expected. Third, the peaks in the histograms for the ferromagnetic metals are much broader (especially for the minority spins) than for Au. This is due to the higher sensitivity of the *d* bands to the atomic positions, as compared to the *s* orbitals that dominate the transport in the case of Au. This higher sensitivity is a result of the anisotropic spatial dependence of the *d* orbitals.

In addition, we have calculated the values of the current polarization P for each realization of disorder in the contacts. The resulting histograms can be found as insets in the panels of Fig. 5. The peaks in each histogram are centered around the polarization values of the corresponding ideal geometries of Sec. III.

To end this section, we would like to make the following comment. In this work, we have analyzed the conductance of some ideal one-atom geometries and the influence of disorder. These types of calculations are very valuable to elucidate the nature of the electrical conduction in atomic wires. However, one has to be cautious in establishing a direct comparison between such theoretical results and the experiments because of the lack of knowledge of the exact geometries realized experimentally. Ideally, the theory should aim at describing the conductance histograms, which contain the full experimental information without any selection of the data. This is precisely what we have done for Ni contacts in our recent work[55] and we refer the reader to it for further details.

V. CONCLUSIONS

In this work, we have presented a theoretical analysis of the conductance of one-atom-thick contacts of the ferromagnetic 3*d* metals Fe, Co, and Ni. Our calculations are based on

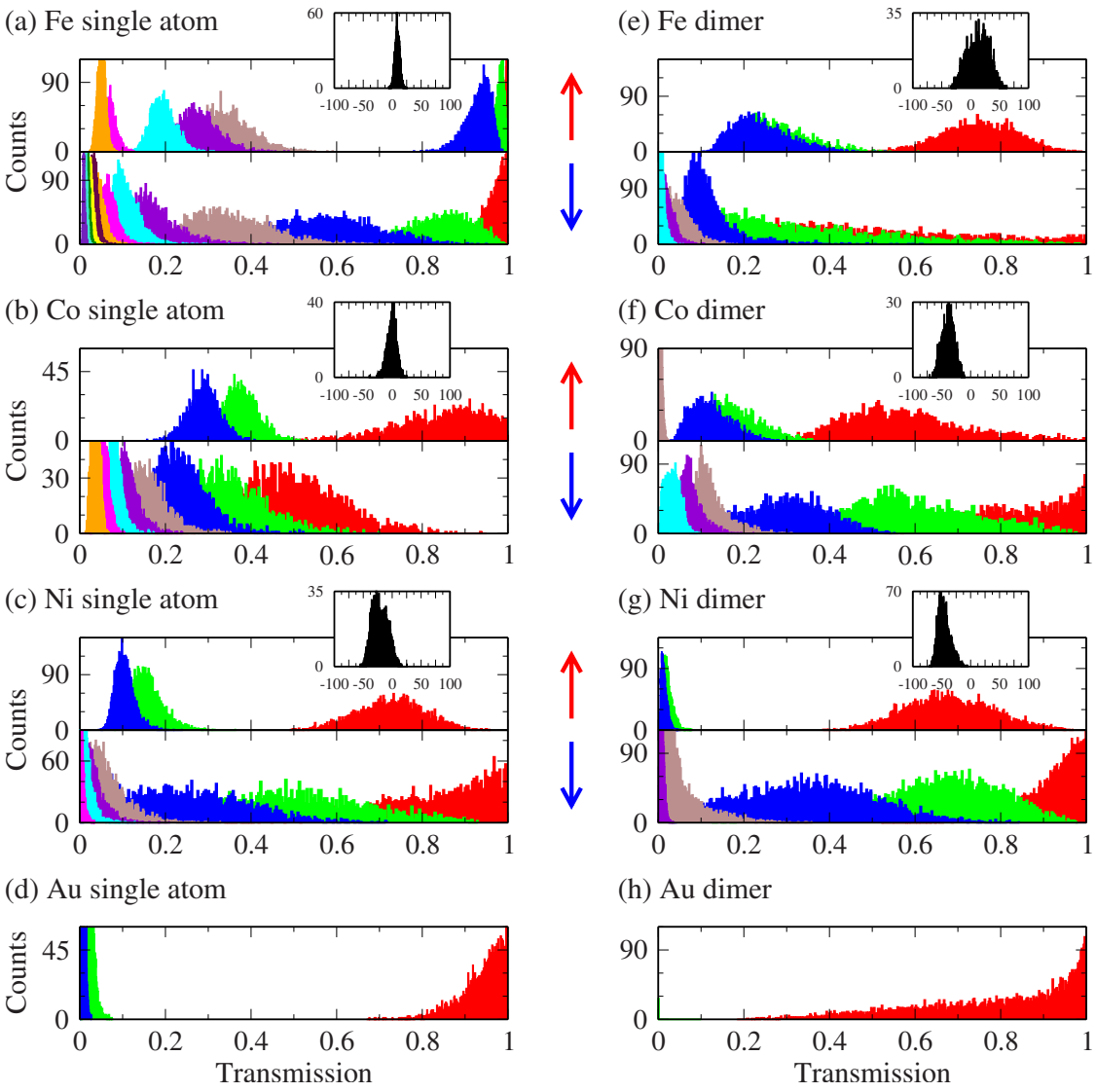

FIG. 5. (Color online) Histograms of transmission channels at Fermi energy, $T_{n,\sigma}(E_F)$, for 3000 perturbed realizations of ideal contact geometries of Fe, Co, and Ni. (a)–(d) show histograms for contacts with a single central atom as in Fig. 2, and (e)–(h) for contacts with a central dimer as in Fig. 3. In (a)–(c) and (e)–(g), results for ferromagnetic contacts are presented: the upper parts of the panels refer to majority spin channels and the lower parts to minority spin channels. Only channels that contribute more than 0.01 to transmission are displayed, and the histograms for smaller transmission values are in the front. The insets for the ferromagnetic materials show corresponding histograms for the current polarization P, where on the x axis P is given in %. Finally, (d) and (h) show comparison histograms for fcc-Au calculated with a similar set of geometries as for Ni.

a self-consistent tight-binding model that has previously been successful in describing the electrical conduction in nonmagnetic atomic-sized contacts. Our results indicate that the d orbitals of these transition metals play a fundamental role in the transport, especially for the minority-spin species. In the case of one-atom contacts, these orbitals combine to provide several partially open conduction channels, which has the following important consequences. First, there is no conductance quantization, neither integer nor half-integer. Second, the current in these junctions is, in general, not fully spin polarized. Third, the conductance of the last plateau is typically above G_0. Finally, both the conductance and the spin polarization of the current are very sensitive to the contact geometry. The ensemble of these theoretical findings supports the recent observations of Untiedt *et al.*,[23] while it is in clear contradiction with the observations of half-integer conductance quantization.[17–22] Of course, the appearance of the quantization in those experiments still remains to be understood. A possible explanation has been put forward by Untiedt *et al.*,[23] who suggested that it could be explained by the presence of contaminants like foreign molecules at the surfaces of the studied samples.

It is interesting to mention that in the tunneling regime, when the contacts are actually broken, the nature of the conduction changes radically. We have shown that, in this case, the transport is mainly dominated by the s orbitals and the spin polarization of the current can reach values close to +100%.

We want to stress that in all our calculations, we have assumed that the atomic contacts were formed by single magnetic domains. In this sense, it would be interesting to see how the conductance in these calculations is modified by the presence of domain walls in the contact region. The first theoretical studies[33,35,37,38] along these lines show that the presence of a domain wall cannot conclusively explain the appearance of huge magnetoresistance values reported in the literature.[13]

Recently, the so-called anisotropic magnetoresistance has been observed in ferromagnetic atomic contacts.[16,28,30] This effect, i.e., the dependence of the resistance on the relative alignment of the current and the magnetization, stems from the spin-orbit coupling and can give rise to a correction to the resistance on the order of 1% in bulk ferromagnets.[63] Although the correction can be bigger for atomic-sized contacts,[29,30,64] it is, nevertheless, expected to be a relatively small effect. The main ingredient that determines the conduction in the 3*d* ferromagnets is the electronic structure, which is what we have described in this work.

ACKNOWLEDGMENTS

We thank Elke Scheer, Magdalena Hüfner, Sören Wohlthat, and Michel Viret for helpful discussions. M.H., J.K.V., F.P., and J.C.C. were supported financially by the Landesstiftung Baden-Württemberg within the "Kompetenznetz Funktionelle Nanostrukturen," the Helmholtz Gemeinschaft within the "Nachwuchsgruppen-Programm" (Contract No. VH-NG-029), and the DFG within the CFN. M.H. acknowledges financial support by the Karlsruhe House of Young Scientists. D.F. was supported by the European Commission through the Research Training Network (RTN) "Spintronics." M.D. and P.N. appreciate the support by the SFB 513.

[1] N. Agraït, A. Levy Yeyati, and J. M. van Ruitenbeek, Phys. Rep. **377**, 81 (2003).
[2] J. C. Cuevas, A. Levy Yeyati, and A. Martín-Rodero, Phys. Rev. Lett. **80**, 1066 (1998).
[3] E. Scheer, N. Agraït, J. C. Cuevas, A. Levy Yeyati, B. Ludoph, A. Martín-Rodero, G. Rubio, J. M. van Ruitenbeek, and C. Urbina, Nature (London) **394**, 154 (1998).
[4] J. C. Cuevas, A. Levy Yeyati, A. Martín-Rodero, G. Rubio Bollinger, C. Untiedt, and N. Agraït, Phys. Rev. Lett. **81**, 2990 (1998).
[5] B. Ludoph, N. van der Post, E. N. Bratus', E. V. Bezuglyi, V. S. Shumeiko, G. Wendin, and J. M. van Ruitenbeek, Phys. Rev. B **61**, 8561 (2000).
[6] C. Sirvent, J. G. Rodrigo, S. Vieira, L. Jurczyszyn, N. Mingo, and F. Flores, Phys. Rev. B **53**, 16086 (1996).
[7] J. L. Costa-Krämer, Phys. Rev. B **55**, R4875 (1997).
[8] K. Hansen, E. Laegsgaard, I. Stensgaard, and F. Besenbacher, Phys. Rev. B **56**, 2208 (1997).
[9] F. Ott, S. Barberan, J. G. Lunney, J. M. D. Coey, P. Berthet, A. M. de Leon-Guevara, and A. Revcolevschi, Phys. Rev. B **58**, 4656 (1998).
[10] H. Oshima and K. Miyano, Appl. Phys. Lett. **73**, 2203 (1998).
[11] T. Ono, Y. Ooka, H. Miyajima, and Y. Otani, Appl. Phys. Lett. **75**, 1622 (1999).
[12] F. Komori and K. Nakatsuji, J. Phys. Soc. Jpn. **68**, 3786 (1999).
[13] N. García, M. Muñoz, and Y.-W. Zhao, Phys. Rev. Lett. **82**, 2923 (1999).
[14] B. Ludoph and J. M. van Ruitenbeek, Phys. Rev. B **61**, 2273 (2000).
[15] A. I. Yanson, Ph.D. thesis, Universiteit Leiden, 2001.
[16] M. Viret, S. Berger, M. Gabureac, F. Ott, D. Olligs, I. Petej, J. F. Gregg, C. Fermon, G. Francinet, and G. Le Goff, Phys. Rev. B **66**, 220401(R) (2002).
[17] F. Elhoussine, S. Mátéfi-Tempfli, A. Encinas, and L. Piraux, Appl. Phys. Lett. **81**, 1681 (2002).
[18] M. Shimizu, E. Saitoh, H. Miyajima, and Y. Otani, J. Magn. Magn. Mater. **239**, 243 (2002).
[19] D. Gillingham, I. Linington, and J. Bland, J. Phys.: Condens. Matter **14**, L567 (2002).
[20] V. Rodrigues, J. Bettini, P. C. Silva, and D. Ugarte, Phys. Rev. Lett. **91**, 096801 (2003).
[21] D. Gillingham, C. Müller, and J. Bland, J. Phys.: Condens. Matter **15**, L291 (2003).
[22] D. Gillingham, I. Linington, C. Müller, and J. Bland, J. Appl. Phys. **93**, 7388 (2003).
[23] C. Untiedt, D. M. T. Dekker, D. Djukic, and J. M. van Ruitenbeek, Phys. Rev. B **69**, 081401(R) (2004).
[24] M. Gabureac, M. Viret, F. Ott, and C. Fermon, Phys. Rev. B **69**, 100401(R) (2004).
[25] C.-S. Yang, C. Zhang, J. Redepenning, and B. Doudin, Appl. Phys. Lett. **84**, 2865 (2004).
[26] J. L. Costa-Krämer, M. Díaz, and P. A. Serena, Appl. Phys. A: Mater. Sci. Process. **81**, 1539 (2005).
[27] K. I. Bolotin, F. Kuemmeth, A. N. Pasupathy, and D. C. Ralph, Nano Lett. **6**, 123 (2006).
[28] Z. K. Keane, L. H. Yu, and D. Natelson, Appl. Phys. Lett. **88**, 062514 (2006).
[29] K. I. Bolotin, F. Kuemmeth, and D. C. Ralph, Phys. Rev. Lett. **97**, 127202 (2006).
[30] M. Viret, M. Gabureac, F. Ott, C. Fermon, C. Barreteau, G. Autes, and R. Guirardo-Lopez, Eur. Phys. J. B **51**, 1 (2006).
[31] A. Martín-Rodero, A. Levy Yeyati, and J. C. Cuevas, Physica C **352**, 67 (2001).
[32] P. S. Krstić, X.-G. Zhang, and W. H. Butler, Phys. Rev. B **66**, 205319 (2002).
[33] A. Smogunov, A. Dal Corso, and E. Tosatti, Surf. Sci. **507**, 609 (2002); **532**, 549 (2003).
[34] A. Delin and E. Tosatti, Phys. Rev. B **68**, 144434 (2003).
[35] J. Velev and W. H. Butler, Phys. Rev. B **69**, 094425 (2004).
[36] A. R. Rocha and S. Sanvito, Phys. Rev. B **70**, 094406 (2004).
[37] A. Bagrets, N. Papanikolaou, and I. Mertig, Phys. Rev. B **70**, 064410 (2004).
[38] D. Jacob, J. Fernández-Rossier, and J. J. Palacios, Phys. Rev. B **71**, 220403(R) (2005).

[39] M. Wierzbowska, A. Delin, and E. Tosatti, Phys. Rev. B **72**, 035439 (2005).
[40] H. Dalgleish and G. Kirczenow, Phys. Rev. B **72**, 155429 (2005).
[41] P. A. Khomyakov, G. Brocks, V. Karpan, M. Zwierzycki, and P. J. Kelly, Phys. Rev. B **72**, 035450 (2005).
[42] J. Fernández-Rossier, David Jacob, C. Untiedt, and J. J. Palacios, Phys. Rev. B **72**, 224418 (2005).
[43] A. Smogunov, A. Dal Corso, and E. Tosatti, Phys. Rev. B **73**, 075418 (2006).
[44] D. Jacob and J. J. Palacios, Phys. Rev. B **73**, 075429 (2006).
[45] K. Xia, M. Zwierzycki, M. Talanana, P. J. Kelly, and G. E. W. Bauer, Phys. Rev. B **73**, 064420 (2006).
[46] A. R. Rocha, T. Archer, and S. Sanvito, Phys. Rev. B **76**, 054435 (2007).
[47] J. C. Tung and G. Y. Guo, Phys. Rev. B **76**, 094413 (2007).
[48] A. Bagrets, N. Papanikolaou, and I. Mertig, Phys. Rev. B **75**, 235448 (2007).
[49] D. J. Bakker, Y. Noat, A. I. Yanson, and J. M. van Ruitenbeek, Phys. Rev. B **65**, 235416 (2002).
[50] G. Autès, C. Barreteau, D. Spanjaard, and M. C. Desjonquères, J. Phys.: Condens. Matter **18**, 6785 (2006).
[51] M. J. Mehl and D. A. Papaconstantopoulos, Phys. Rev. B **54**, 4519 (1996).
[52] M. Häfner, P. Konrad, F. Pauly, J. C. Cuevas, and E. Scheer, Phys. Rev. B **70**, 241404(R) (2004).
[53] J. K. Viljas, J. C. Cuevas, F. Pauly, and M. Häfner, Phys. Rev. B **72**, 245415 (2005).
[54] M. Dreher, F. Pauly, J. Heurich, J. C. Cuevas, E. Scheer, and P. Nielaba, Phys. Rev. B **72**, 075435 (2005).
[55] F. Pauly, M. Dreher, J. K. Viljas, M. Häfner, J. C. Cuevas, and P. Nielaba, Phys. Rev. B **74**, 235106 (2006).
[56] M. Brandbyge, N. Kobayashi, and M. Tsukada, Phys. Rev. B **60**, 17064 (1999).
[57] N. C. Bacalis, D. A. Papaconstantopoulos, M. J. Mehl, and M. Lach-hab, Physica B **296**, 125 (2001).
[58] F. Guinea, C. Tejedor, F. Flores, and E. Louis, Phys. Rev. B **28**, 4397 (1983).
[59] D. R. Lide, *CRC Handbook of Chemistry and Physics*, 79th ed. (CRC, Boca Raton, FL, 1998).
[60] A. Messiah, *Quantum Mechanics* (Wiley, New York, 1958), Vol. 1.
[61] P. Jelínek, R. Pérez, J. Ortega, and F. Flores, Phys. Rev. B **68**, 085403 (2003).
[62] R. J. Soulen, Jr., J. M. Byers, M. S. Osofsky, B. Nadgorny, T. Ambrose, S. F. Cheng, P. R. Broussard, C. T. Tanaka, J. Nowak, J. S. Moodera, A. Barry, and J. M. D. Coey, Science **282**, 85 (1998).
[63] T. R. Mcguire and R. I. Potter, IEEE Trans. Magn. **11**, 1018 (1975).
[64] J. Velev, R. F. Sabirianov, S. S. Jaswal, and E. Y. Tsymbal, Phys. Rev. Lett. **94**, 127203 (2005).